Article

JOURNAL OF REINFORCED PLASTICS & COMPOSITES

Journal of Reinforced Plastics and Composites
32(5) 289–299

DOI: 10.1177/0731684412471091
jrp.sagepub.com
SAGE

Quasi-static behavior of three-dimensional integrated core sandwich composites under compression loading

Mehmet Karahan[1], Nevin Karahan[1], Hakan Gul[1] and Jan Ivens[2,3]

Abstract

In the current study, the effect of the thickness and the foam density in three-dimensional integrated woven sandwich composites on quasi-static properties was investigated. For this purpose, produced samples were subjected to uniaxial flatwise compression tests and their compression strength and moduli were determined. Obtained results were optimized by taking core thickness, foam density and panel weights into consideration. Damages that occurred on the tested samples were reported. When compared to conventional foam core sandwich composites, it was found that three-dimensional integrated sandwich composites have better compression properties and due to the fact that the pile yarns in the core and the foam support each other.

Keywords

Three-dimensional integrated sandwich composites, quasi-static properties, damage tolerance

Introduction

Sandwich composites are used in different areas such as automotive, aerospace, marine and construction industry, and with a wide variety since they combine light weight with high flexural properties. Conventional sandwich structures are made of two skin layers with high modulus and a low-density core material between these layers such as metallic and non-metallic honeycomb, polyurethane and polyvinyl chloride foam, balsa and corrugated core, and the skins and core materials are adhered to each other.[1] The most significant disadvantage of sandwich composites is the low skin-core interface adhesion. Therefore, a great deal of attention has to be paid to the prevention of delaminations between skins and core occurring in conventional sandwich materials under load.[2] Furthermore, the core essentially has to have the adequate stiffness and strength in order to bear loads (particularly compression and shear loads) without any significant level of deformation or damage. Also, the production costs of sandwich composite materials have to be taken into consideration in material design.

Stitching and Z-pinning[3,4] can be described as the most important examples among the new production techniques developed in order to create a solution for the inadequacies of conventional sandwich materials. These techniques used in foam-filled sandwich materials improve through the thickness properties and particularly impact resistance and damage tolerance. However, due to the reinforcements between the facesheets in both methods, some degradation of in-plane properties is generally observed.[5] Furthermore, production of structures with complex forms is very difficult with stitching and pinning methods.

Three-dimensional (3D) textile production methods have led to interesting developments in the composites industry.[6–9] The use of 3D integrated fabrics in the

[1]University of Uludag Vocational School of Technical Sciences, Gorukle Bursa, Turkey
[2]University of Leuven, Department of Metallurgy and Materials Engineering, Leuven, Belgium
[3]University of Leuven – Thomas More, Department of Engineering Technology, Sint-Katelijne-Waver, Belgium

Corresponding author:
Mehmet Karahan, University of Uludag Vocational School of Technical Sciences, Gorukle Bursa, Turkey.
Email: mkarahan@uludag.edu.tr

production of sandwich composites has presented a new concept on this topic.[10–12] 3D integrated sandwich fabrics are made by the velvet carpet weaving technique, where two parallel skins (top and bottom skins) are woven together using pile yarns,[11] keeping a defined distance between the skins to form a core. This integrated connection provides a through-the-thickness reinforcement, in which the pile yarn architecture increases the shear rigidity, which is the most significant disadvantage of many core materials.[13,14] The warp and weft yarns constitute the skins while the pile yarns create a hollow core section, the pile yarn free length determining the core thickness. This sandwich fabric structure has the following advantages: (1) sandwich panels can be produced in a single step, production costs are reduced in line with the shortened production time, (2) top and bottom skins are integrally woven together with the core section and this ensures a stronger binding between the layers: skin-core delamination is virtually impossible, (3) the hollow core section can be filled by several means, thus different functional capabilities can be given to the structure.

There are several studies available on 3D woven sandwich production processes and properties.[15,16] Some researchers examined the mechanical properties of 3D sandwich composites.[17–20] They found that 3D sandwich composites have a high skin-core delamination resistance and the pile yarns have a significant influence on flatwise compression and shear properties. Shiah et al.[21] examined the elastic modulus and impact properties of 3D integrated sandwich composites. Wang et al.[22] focused on the 3-point bending and flatwise compression properties of multi-face sheet 3D integrated sandwich composites and reported that such structures have superior mechanical properties than mono-spacer 3D sandwich composites. In another study, Wang et al.[23] determined the bending, compression and shear properties of 3D sandwich composites for different foam densities. Brandt et al.[24] examined the planar properties (strength and modulus), damage properties, energy absorption capacities and mechanical breakage properties of different three-dimensioned woven composites. Van Vuure et al.[13,25] focused on strength and modulus properties on an empirical and simulative way. 3D sandwich fabrics constitute a good potential for the production of multi-functional composites.[26] Researchers[27–29] also studied other properties of woven textile sandwich composites such as fatigue, damage and low-velocity impact properties: in a study,[30] woven textile sandwich composites were compared with honeycomb sandwiches. The results showed that the properties of 3D woven sandwich composites are better in the weft direction compared to the warp direction.

Compression, bending and impact properties of 3D woven sandwich composites are quite low without any extra skin reinforcement. Also core shearing resistance decreases as the pile height increases. Due to this, core sections of these materials are generally filled with foam, although it causes a weight increase.[13–17] Change of core thickness and use of foam filling in the core significantly affects the mechanical properties.[12,31,32] Furthermore, core thickness and the use of foam filling require the simultaneous optimization of mechanical properties and weight.

In the present study, 3D sandwich composites with varying core thicknesses were filled with foam of varying densities and the effects of the changes in thickness and foam density on quasi-static properties were examined. For this purpose, produced samples were subjected to uniaxial flatwise compression tests and their compression strength and moduli were determined.

Materials and experimental methods

3D integrated fabrics

The 3D sandwich fabrics have been supplied by Parabeam BV (NL). The 3D integrated fabrics used in the research had a core thickness of 10, 15, 18 and 22 mm. All four fabrics are identical in terms of their top and bottom skin layers, the yarns used and the weaving architecture. The only difference is their free pile yarn length and thus the core thickness. Figure 1 illustrates the layout of the yarns in the structure and a typical weaving architecture of a 3D integrated sandwich fabric. It shows that binding yarns connect the top and bottom skins of the structure in thickness direction and consequently the core of the fabric becomes hollow. The parameters of the fabrics used in the study are given in Table 1. All yarns consist of type E glass fibres. The linear density of the warp, weft and pile yarns is 300 tex.

The structure of 3D integrated sandwich fabrics is different from conventional woven fabrics.[33] Therefore, the fabric geometry was established based on the yarn intersections within the fabrics, to understand the fabric structure and geometry, and from basic parameters such as yarn width, yarn thickness, weave densities and yarn spacing. The drawings have been carried out with the Katia CAD program. The schematic display of the 3D fabric structure is presented in Figure 1(c).

The top and bottom skins of sandwich panels have been reinforced with an additional plain weave E-glass fabric. Three additional plain woven fabric layers of 500 g/m^2 were used in both the top and bottom skins during composite production.

Fabrication of 3D integrated core sandwich panels

3D integrated sandwich composites were produced from 3D integrated sandwich fabrics. An Atlac 580

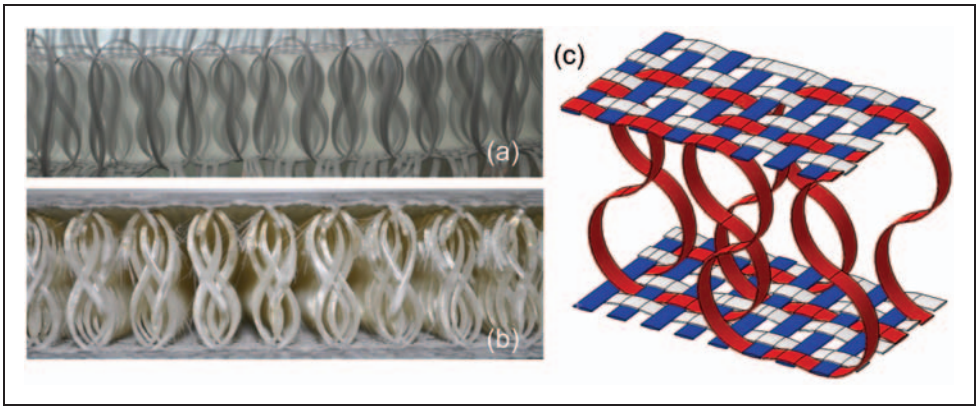

Figure 1. Cross-sectional view of three-dimensional (3D) dry fabric (a) and resin impregnated plate (b); the schematic display of the 3D fabric structure.

Table 1. Main properties of the three-dimensional (3D) fabrics and composite plates

Core thickness (mm)	3D dry fabric (g/m^2)	Total dry fabric (g/m^2)	Fibre volume fraction in fabric (%)	3D composite core thickness (mm)	3D composite plate thickness with additional face sheets (mm)
22 mm	1680	4680	36	22,1	24
18 mm	1720	4720	36	18	19,5
15 mm	1600	4600	36	14,9	16,3
10 mm	1430	4430	35	10,1	12

AC 300 type vinylester urethane resin was used. A 6% cobalt naphthalate accelerator was added in a ratio of 0.25 phr. A 50% active methyl ethyl kethone peroxide catalyst was used with a mixing ratio of 2 phr The vinylester resin has a Young's modulus of 3 GPa and 3.4% strain to failure.

All test panels were manufactured using the hand lay-up technique. Production of the panels has been carried out on a glass plate, treated with a release agent. Special care was taken to control the fibre volume fraction during the production of each panel. The top and bottom skins of the panel have been reinforced with an additional plain weave glass fabric. With this purpose the top and bottom skins of the panels have been reinforced with additional three plies fabric. After applying the resin to the skins from both sides, it has been ensured that the resin thoroughly penetrated the entire fabric and that all entrapped air was removed using aluminum impregnation rollers (Figure 2(a) and (b)).

After the application of the resin, the fabrics have been kept for 4 hours at room temperature for curing. During this time, the impregnated fabric opens up due to the way the pile yarns are woven into the skins. The additional plain weave fabrics have been bonded to the top and bottom skins after the 3D panels have cured with same resin by using hand lay-up. The additional skins cannot be co-laminated as their weight would affect the core thickness. Therefore, the additional fabric layers are laminated onto the sandwich panel after the curing of the 3D sandwich panels. Subsequently, the panels were kept for 1 day for complete curing and specimens were cut from them. The appearances of the plates are shown in Figure 2(c).

The weights of the plates and the weight ratio of fiber and resin of each plate were determined. Since the core sections are hollow, the fiber weight ratios have been determined rather than fiber volume fraction. Table 2 shows the resin and fabric ratios separately for plates of different thicknesses.

Foam filling of 3D integrated core sandwich composites

Some of the panel core sections were filled with rigid polyurethane (PUR) foam, consisting of a mix of 1.08 g/cm^3 polyol and 1.23 g/cm^3 isocyanate (MDI), in a 107/100 isocyanate-polyol mixing ratio (by weight). The foaming process was performed in a mould. During the foam expansion, a pressure of approximately 0.5 bar was built up. A constant temperature of 50°C

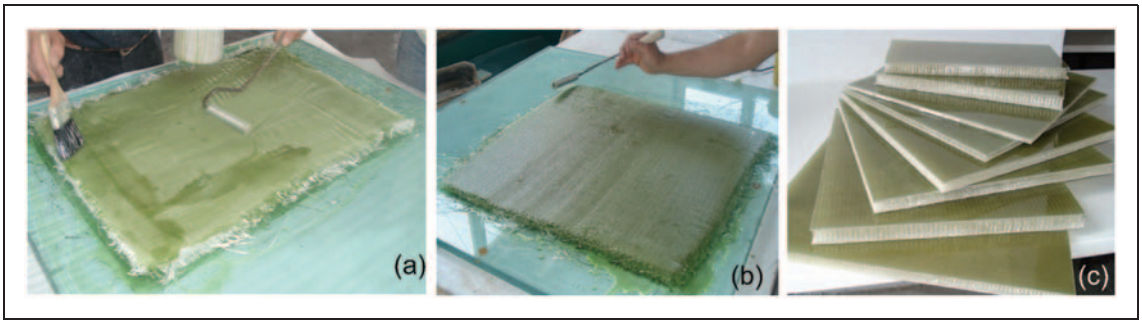

Figure 2. Fabrication of three-dimensional (3D) integrated panels (a and b) and view of finished plates (c).

Table 2. Finished properties of sandwich samples and their sample codes

Core thickness (mm)	Sample code	Foam filling	Density of foam filling (kg/m^3)	Weight ratio of fabric/resin/foam (%)	Unit weight of finished plates (g/m^3)	Weight ratio difference due to foam filling (%)
10	A1	No	–	64/36/0	6710	–
	A2	Yes	100	57/32/11	7550	12.5
	A3	Yes	120	59/27/14	7762	15.7
	A4	Yes	130	58/27/15	7810	16.4
15	B1	No	–	65/35/0	6981	–
	B2	Yes	100	56/29/15	8262	18.3
	B3	Yes	120	54/28/18	8532	22.2
	B4	Yes	130	53/27/20	8647	23.9
18	C1	No	–	65/35/0	7173	–
	C2	Yes	100	51/27/22	8760	22.1
	C3	Yes	120	52/28/20	9076	26.5
	C4	Yes	130	50/28/22	9218	28.5
22	D1	No	–	64/36/0	7088	–
	D2	Yes	100	51/24/25	9283	31
	D3	Yes	120	49/27/24	9695	36.8
	D4	Yes	130	49/24/27	9839	38.8

is maintained throughout the process to enhance the foam penetration between the pile yarns and the homogenity of the foam. The process of injecting foam into the composite plates in the mold is shown in Figure 3. The appearance of the obtained plates with and without foam filling are shown in Figure 3(c). In the end, samples of four different thicknesses (foamed and unfoamed) are obtained. The names of the produced 3D sandwich samples are given in Table 2.

Experimental studies

Flat wise compression tests. Flat wise compression tests were conducted in accordance with ASTM C 365-03. 3D woven sandwich panel was subjected to compression loading in the thickness direction (Figure 4). Compression strength was calculated from the peak load. The compressive strain was obtained from the cross-head displacement, conform with an earlier study.[13]

Following equations were used for calculating compression strength (σ_C) and modulus (E_C).

$$\sigma_C = \frac{P_U}{A} \tag{1}$$

$$E_C = \frac{\sigma_C}{(w/h)} \tag{2}$$

Here, P_U is the maximum load, A is the area, w is the cross-head displacement and h is the sample thickness.

Compression tests were carried out by compressing the sample in the thickness direction between two parallel plates. Circular plates of 100 mm diameter were used for the test. The samples were cut to a dimension

Figure 3. Fabrication steps of foam filling process (a and b) and view of foamed and unfoamed panels (c).

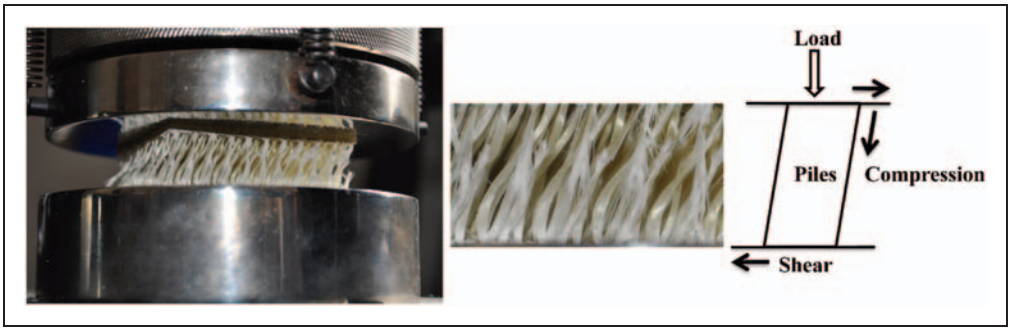

Figure 4. View of flatwise compression test fixtures and mixed mode loading due to sliding during compression of inclined piles.

of $60 \times 60\,mm^2$ and positioned between the clamps with the warp direction facing the front. A 4411 model instron equipment of 5 kN capacity was used for the tests. The cross-head displacement rate was 1 mm/min. Each test was conducted with at least four samples.

Results and discussion

Flatwise compression tests were applied as shown in Figure 4. The tests were carried out on samples cut in a square form of $60 \times 60\,mm^2$. As shown in Figure 4, the reduction in thickness resulted in core shear deformation in combination with core compression. The somewhat inclined form of the pile yarns, present after panel production, causes the shear deformation to be more dominant, especially in samples without foam filling, and with increasing core thickness. Consequently, one of the skin layers starts to slide away and the compression force becomes friction-dependant. In order to prevent this anomaly, the skins were fixed to the loading plates, resulting in a higher and more accurate compression value. With decreasing core thickness and increasing foam density, the core shear resistance increases and accordingly shear deformations decrease. Compression strength and modulus were calculated with the use of equations (1) and (2). Results are presented in Table 3.

Typical compressive stress–strain curves for the different sandwich composites are presented in Figure 5. The curves show how the compression behavior changes with changing core thickness, foam filling and foam-filling density. The stress–strain behavior of 3D sandwich composites under compression load can be generalized as follows: (1) an elastic region that is initially linear then becoming non-linear up to a first maximum in the curve, after which the load drops, (2) a plateau corresponding to a gradual core crushing at almost constant stress and (3) the section where the stress increases rapidly due to core densification. These three regions were reported by other researchers.[34,35]

The compression strength in unfoamed samples is based only on the compression load-bearing capacity of the pile yarns. However, pile yarns are easily subjected to shear deformation and exhibit a low compression strength, particularly with increasing core thickness. In the elastic region, the pile yarns undergo minor deformations while being compressed. Once the peak load is reached, the stress falls rapidly: at this point pile buckling deformation takes place first, followed by the onset of shear deformation. In the following process, pile rupture takes place due to the bending and buckling during a long plateau where the stress remains nearly constant. The length of the plateau depends on the pile length. As the core density

Table 3. Flat-wise compression test results

Samples	Modulus (GPa)	Peak stress (MPa)	Unit weight of samples (kg/m^3)	Specific modulus GPa·m^3·kg^{-1}	Specific strength MPa· m^3·kg^{-1}
A1	0.479 ± 0.090	1.027 ± 0.096	6.710	0.0714	0.0153
A2	0.678 ± 0.044	1.580 ± 0.140	7.550	0.0875	0.2040
A3	0.770 ± 0.055	1.670 ± 0.106	7.762	0.0992	0.2150
A4	0.860 ± 0.110	1.740 ± 0.180	7.810	0.1101	0.2230
B1	0.350 ± 0.037	0.680 ± 0.120	6.981	0.0501	0.0970
B2	0.520 ± 0.080	1.120 ± 0.180	8.262	0.0629	0.1360
B3	0.600 ± 0.049	1.240 ± 0.150	8.532	0.0703	0.1450
B4	0.720 ± 0.043	1.420 ± 0.120	8.647	0.0833	0.1640
C1	0.188 ± 0.074	0.336 ± 0.043	7.173	0.0262	0.0470
C2	0.370 ± 0.036	0.940 ± 0.068	8.760	0.0422	0.1070
C3	0.520 ± 0.024	1.070 ± 0.059	9.076	0.0573	0.1180
C4	0.580 ± 0.100	1.240 ± 0.160	9.218	0.0629	0.1350
D1	0.134 ± 0.014	0.266 ± 0.018	7.088	0.0190	0.0380
D2	0.340 ± 0.055	0.750 ± 0.057	9.283	0.0366	0.0810
D3	0.460 ± 0.050	0.960 ± 0.035	9.695	0.0474	0.0990
D4	0.500 ± 0.042	1.100 ± 0.123	9.839	0.0508	0.1120

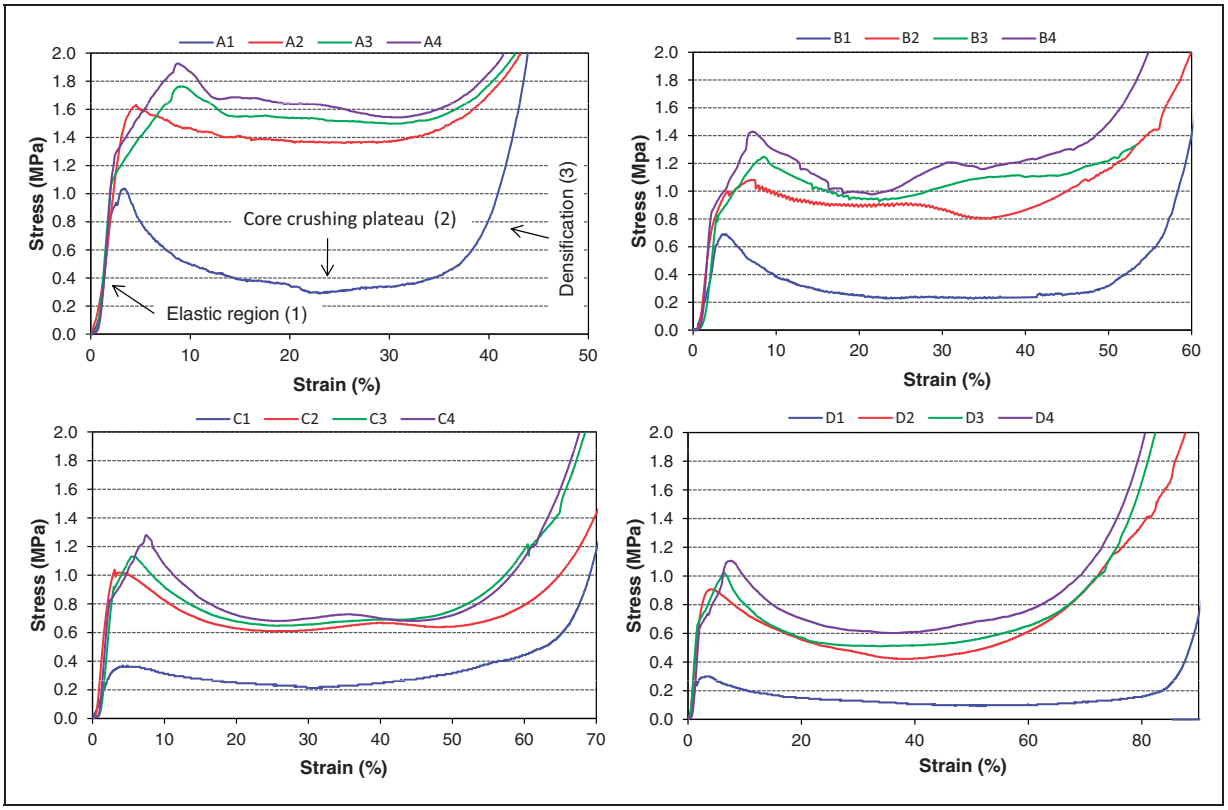

Figure 5. Stress–strain graphs of different samples under compression loading based on the change in foam density.

increases, pile yarns in the core start to contact each other and the stress rises rapidly.

Pile yarns under compressive load easily bend due to their 8 shape, at the same time some of the pile yarns rupture at the entrance in the upper or bottom skins, while others rupture at or close to the contact points in the middle. While the ruptures taking place at the skin connection points cause the complete failure of the pile yarn, the fracture at the mid-sections are often partial (Figure 6). When the compressive load is lifted, the unfoamed sandwich structure partially recovers. As the core thickness increases the peak compressive load decreases. The peak load is related to the pile buckling, the buckling force is inversely proportional to the square of free or unsupported pile length. Plateau length increases with increasing core thickness.

Foam-filled sandwich composites display an elastic region of approximately 0–2% strain. The behavior of the foamed sandwich panels is similar to the behavior of cellular solid materials.[36] However, the foam-filled panels first experience deformation due to the elastic bending of the foam cell struts and walls and the pile yarns, followed by buckling of struts, walls and piles. As a result of this, the stress–strain curve of foam-filled composites has a long plateau where the compressive stress is nearly constant. Air voids formed within foam filling do not exhibit a homogenous distribution. These air voids are the weakest points of the structure and plastic deformation starts with the rupture of these parts.[37] The rate of air voids within the foam decreases with higher foam density and accordingly the crushing plateau somewhat shortens. After the compressed structure reaches a certain level of compaction, the stress increases rapidly. Beyond this point, the core behaves as a solid.

Visual observation carried out during the tests showed that the cracking of foam core starts from the middle of the core and later spreads to upper and lower parts. This was also observed by other researchers.[38] The damage behavior of the unfoamed panels show that pile rupture occurred at the skins or in the middle of the core. Since the foam density is lower in the center of the core, the support of the pile yarns is less in the middle section. Consequently, damage initiates in the middle section of the core.

As the foam density increases in the samples, the ratio of the peak stress over the plateau stress decreases. Also, the crushing plateau shortens and densification starts earlier. As the foam density increases, shear deformation decreases and compression stress increases depending on the increase in core shear resistance. However, shear is not prevented completely, the longer piles are weaker in compression, that is why the reinforcing effect of the piles goes down. Comparing the compression behavior of foam cores to those of honeycomb and balsa cores available in the literature,[39,40] some characteristic differences are found. As in foam core, honeycomb core sandwich composites compression behavior exhibits three areas. However, some differences occur depending on the density of honeycomb core. In low-density honeycomb sandwich composites, buckling deformation takes place earlier and the compression behavior is similar to that of foam cores. However, in medium and high-density honeycomb composites, stress decreases rapidly at the end of the linear elastic region.[40] This is due to the fact that cell walls in honeycomb break instantly when load-bearing capacity is exceeded. The is also the case for balsa cores and since balsa has a higher rigidity it displays this behavior more clearly.[39] The results of this study show that no instant breakage takes place even with high-density foam cores. This signifies the capability of foam core to take its previous form when the load is removed at elastic region and it was verified by the study of Koissin and Shipsha[41] that examined the

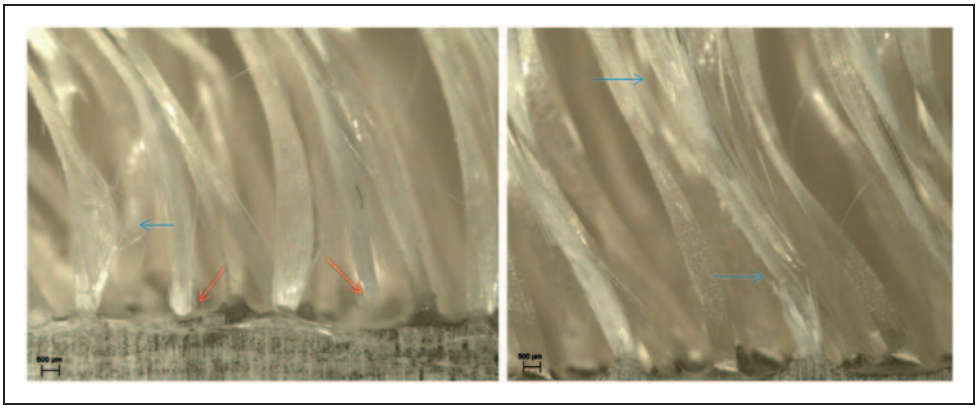

Figure 6. Broken pile yarns from mid sections (blue arrows) and bottom parts after compression test.

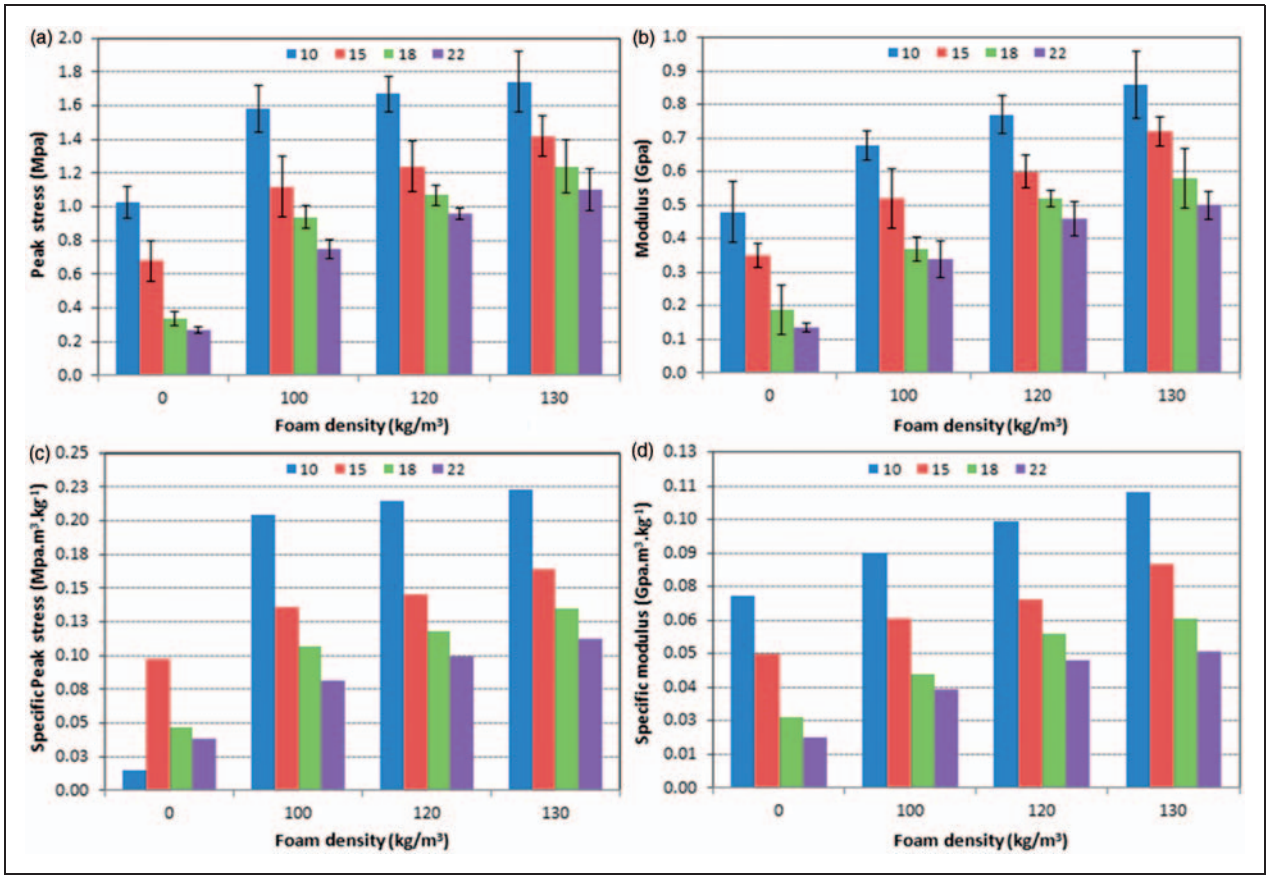

Figure 7. Change of peak stress (a), specific peak stress (c), modulus (b) and specific modulus (d) according to foam density.

relaxation effect by means of repetitive loading tests. In comparison with other core materials, the best property of 3D sandwich composites is their tendency to partially take their original form after the load is removed. This is the result of the form of pile yarns similar to the 8 shape, they act as a spring between the two skins. This effect is larger in structures without foam filling. Therefore, 3D sandwich composites can be accepted as core materials having a perfect elastic behavior.

Table 3 presents the flat-wise compression test results. Comparing the data shows that as the thickness increases from 10 mm to 22 mm for unfoamed samples, peak stress decreases from 1.03 MPa to 0.27 MPa, while compression modulus falls 0.48 GPa to 0.13 GPa. The decreases in peak stress and modulus as the increase of thickness is related to the increase of the unsupported length of pile yarns in the core section. The highest compression modulus in unfoamed samples was found in samples with the lowest thickness (10 mm). The compression strength for unfoamed samples A and B is higher than that of some honeycomb sandwich composites[42] and some lattice truss materials.[43] As for the compression modulus of foamed samples A and B, it is fairly close to that of some foam, honeycomb and lattice truss materials.[42,43]

Comparing the sample with 10 mm core thickness, with 15, 18 and 22 mm core thickness, the peak stress decreases by 34%, 67% and 74%, respectively, while the compression modulus decreases with 27%, 60% and 71%, respectively (Figure 7). In sandwich samples of 10 mm core thickness, peak stress increased by 53–69% when compared with unfoamed sample, while compression modulus increased by 41–79%. For the sample with 15 mm core thickness, peak stress increased by 64–108% while compression modulus increased by 48–105% based on the foam density. For the sample with 18 mm core thickness, peak stress increased by 179–268% while compression modulus increased by 96–208% based on the foam density. As for the sample with 22-mm core thickness, peak load increased by 181–312% while the increases in compression modulus were 152–270% based on the foam density. Figure 7 shows that the foam density positively affects the peak stress and the compression modulus, the effect becoming more pronounced with increasing core thickness. However, the density of the plates increases as well, so it is preferred to evaluate the specific material properties (Figure 7). Table 3 shows the specific peak stress and specific modulus values. Figure 7 shows that also the specific peak stress and modulus

Table 4. Average compression modulus, peak stress, specific compression modulus and specific peak stress values obtained with SNK analysis for different parameters

Parameters	Compression modulus (GPa)	Peak stress (MPa)	Specific compression modulus ($GPa \cdot m^3 \cdot kg^{-1}$)	Specific stress ($MPa \cdot m^3 \cdot kg^{-1}$)
Core thickness (mm)				
10	0.696	1.504	0.314	0.164
15	0.547	1.115	0.279	0.121
18	0.414	0.869	0.120	0.101
22	0.312	0.769	0.092	0.082
Foam density (kg/m^3)				
0	0.287	0.577	0.070	0.049
100	0.477	1.097	0.139	0.117
120	0.541	1.235	0.288	0.144
130	0.665	1.375	0.308	0.158

increase with increasing foam density. Since shear resistance decreases with the increase of core thickness, it is understood that the density of foam has to be higher to increase the compressive strength.

According to the two-factor ANOVA test conducted at 95% confidence level, statistically significant effects of foam density and sample thickness were determined on compression modulus and peak stress values. The same trend was also detected for specific compression modulus and specific strength.

According to this, the results of each factor, obtained with 95% confidence level according to Student Newman Keuls analysis, are shown in Table 4. An arrangement of all of the factors according to their respective average values of compression modulus, peak stress, specific compression modulus and specific peak stress is presented here. The results of this arrangement can give an idea in terms of optimization of the results.

According to these results, in the assessment made for all samples based on core thicknesses, when the samples of 10 mm core thickness is compared to the samples of 15, 18 and 22 mm core thicknesses, respectively, 21%, 41% and 55% higher compression moduli and again, respectively, 26%, 42% and 49% higher peak stress values were obtained. In the assessment made for core thickness on the basis of unit weight, the specific compression moduli of the sample of 10 mm core thickness were obtained 11%, 62% and 72% higher than those of the samples of 15, 18 and 22 mm core thicknesses, while the specific peak stresses of the sample of 10 mm were 26%, 38% and 50% higher than that of the compared samples.

As for the assessment made for all samples on the basis of foam densities, for the samples with densities of 100, 120 and 130 compression modulus values increased by 66%, 88% and 132% in comparison to the unfoamed sample, while the increases in peak stress were 30%, 114% and 138%. For the assessment made on the basis of unit weight, the specific modulus values of samples with densities of 100, 120 and 130 increased by 98%, 311% and 340% in comparison with the unfoamed sample, while the increases in the specific peak stress values were 138%, 194% and 222%. The results indicate that decreases in core thickness and particularly increases of foam densities have dramatic effects on compression modulus and peak stress values.

The compression peak stress decreases with increasing pile length. The compression peak stress increases dramatically by adding foam in the core and increases with increasing core density. The compression modulus increases of up to three times with foam filling. After buckling, the stress–strain curve exhibits a long plateau.

Conclusion

In this study, quasi-static properties of 3D integrated sandwich woven composites under compression loading were examined in terms of the changes in core thickness and foam-filling density, and the following conclusions were obtained.

- The somewhat inclined form of the pile yarns causes compression and shear deformations to occur at the same time in compression tests.
- It can be generally stated that compression peak stress decreases in line with the increase in pile yarn length.
- Compression peak stress increases dramatically in line with the use of foam filling in the core and the increase of foam-filling density. With the use of foam filling, increases of up to three folds were obtained in compression modulus.

- In the assessment made for core thickness on the basis of unit weight, the specific compression moduli of the sample of 10 mm core thickness were obtained 11%, 62% and 71% higher than those of the samples of 15, 18 and 22 mm core thicknesses, while the specific peak stresses of the sample of 10 mm were 26%, 38% and 50% higher than that of the compared samples.
- For the assessment made on the basis of unit weight, the specific modulus values of samples with densities of 100, 120 and 130 increased by 98%, 311% and 340% in comparison with the sample without foam filling, while the increases in the specific peak stress values were 138%, 194% and 222%.
- Under compression loading 3D composites exhibit comparable, and with the use of foam filling even superior properties, from other core materials such as conventional foam core, honeycomb and lattice.

Funding

This study was funded by Uludag University Scientific Research Unit (UAP-TBMYO/2010-32) and Tubitak (109M350).

References

1. Karlsson KF and Astrom T. Manufacturing and application of structural sandwich components. *Compos Part A* 1997; 28A: 97–111.
2. Zenkert D. *The handbook of sandwich construction*. London: Engineering Materials Advisory Chameleon Press, 1997, pp.165–167.
3. Potluri P, Kusak E and Reddy T. Novel stitch-bonded sandwich composite structures. *Compos Struct* 2003; 59: 251–259.
4. Mines RW, Worrall CM and Gibson AG. Low velocity perforation behavior of polymer composite sandwich panels. *Int J Impact Eng* 1998; 21(10): 855–879.
5. Lascoup B, Aboura Z, Khellil K, et al. On the mechanical effect of stitch addition in sandwich panel. *Compos Sci Technol* 2006; 66(10): 1385–1398.
6. Lomov SV, Bogdanovich AE, Ivanov DS, et al. A comparative study of tensile properties of non-crimp 3d orthogonal weave and multi-layer plain weave e-glass composites. Part 1: materials, methods and principal results. *Compos A* 2009; 40: 1134–1143.
7. Ivanov DS, Lomov SV, Bogdanovich AE, et al. A Comparative study of tensile properties of non-crimp 3d orthogonal weave and multi-layer plain weave e-glass composites. Part 2: Comprehensive experimental results. *Compos A* 2009; 40: 1144–1157.
8. Karahan M, Ulcay Y, Eren R, et al. Investigation into the tensile properties of stitched and unstitched woven aramid/vinyl ester composites. *Tex Res J* 2010; 80(10): 880–891.
9. Karahan M, Ulcay Y, Karahan N, et al. Influence of stitching parameters on tensile stregth of aramid/vinyl ester composites. *Mater Sci (Medziagotyra)*, Accepted paper in press (2012).
10. Barrett DJ. A micromechanical model for the analysis of Z-fiber reinforcement. In: *AIAA/ASCE/ASME/AHS SDM Conference*, Salt Lake City, Utah, 1996, AIAA-96-1329-CP, pp.62–67.
11. ZCL Composites Inc. Company Literature. ST. Edmonton, AB. Canada, 1998.
12. Vaidya UK, Hosur MV, Earl D, et al. Impact response of integrated hollow core sandwich composite panels. *Compos: Part A* 2000; 31: 761–72.
13. Van Vuure AW, Pflug J, Ivens J, et al. Modelling the core properties of composite panels based on woven sandwich-fabric preforms. *Compos Sci Technol* 2000; 60: 1263–1276.
14. Judawisastra H, Ivens J and Verpoest I. Determination of core shear properties of 3D woven sandwich composites. *Plast Rubber Compos: Proc Appl* 1999; 28: 452–457.
15. Van Vuure AW, Ivens J and Verpoest I. Sandwich panels produced from sandwich-fabric preforms. In: *Proceeding of the International Symposium on Advanced Materials for Lightweight Structures'94*, ESA_ESTEC Noordwijk Netherlands, 22–25 March 1994, pp.609–12.
16. Van Vuure AW, Ivens J and Verpoest I. Sandwich-fabric panels. In: *Proceedings of the 40th International SAMPE Symposium and Exhibition*. Anaheim convention center, Anaheim California, 8–11 May 1995, pp.996–76.
17. Verpoest I, Wevers M, Ivens J, et al. 3D fabrics for ompression and ımpact resistant composite sandwich structures. In: *Proceedings of the 35th International SAMPE Symposium*. Anaheim convention center, Anaheim California, 2–5 April 1990, pp.296–305.
18. Zic I, Ansell MP, Newton A, et al. Mechanical properties of composite panels reinforced with ıntegrally woven 3D fabrics. *J Text Instit* 1990; 81(4): 461–479.
19. Nakatani T, Nakai A, Fujita A, et al. Mechanical behaviour in glass 3D woven fabric composites. In: *Proceedings of the Fourth Japan International SAMPE Symposium*, Tokyo, Japan, 24–28 September 1995, pp.1473–1478.
20. Bannister MK, Braemar R and Crothers PJ. The mechanical performance of 3D woven sandwich composites. *Compos Struct* 1999; 47: 687–690.
21. Shiah YC, Tseng L, Hsu JC, et al. Experimental characterization of an integrated sandwich composite using 3D woven fabrics as the core material. *J Thermoplast Compos Mater* 2004; 17: 229–243.
22. Wang S, Li M, Zhang Z, et al. Properties of face sheet-reinforced 3-D spacer fabric composites and the integral multi-face sheet structures. *J Reinf Plast Compos* 2010; 29(6): 793–806.
23. Wang B, Wu L, Jin X, et al. Experimental investigation of 3D sandwich structure with core reinforced by composite columns. *Mater Design* 2010; 31: 158–165.
24. Brandt J, Drechsler K and Arendts FJ. Mechanical performance of composites based on various three-dimensional woven-fibre performs. *Compos Sci Technol* 1996; 56: 381–386.
25. van Vuure AW, Ivens JA and Verpoest I. Mechanical properties of composite panels based on woven sandwich-fabric performs. *Compos Part A* 2000; 31: 671–680.

26. van Vuurea AW, Verpoest I and Ko FK. Sandwich-fabric panels as spacers in a constrained layer structural damping application. *Compos Part B* 2001; 32: 11–19.
27. Judawisastra H, Ivens J and Verpoest I. The fatigue behavior and damage development of 3D woven sandwich composites. *Compos Struct* 1998; 43: 35–45.
28. Vaidya UK, Hosur MV, Earl D, et al. Impact response of integrated hollow core sandwich composite panels. *Compos Part A* 2000; 31: 761–72.
29. Karahan M, Gul H, Ivens J, et al. Low velocity impact characteristic of 3D integrated core sandwich composites. *Text Res J* 2012; 82(9): 845–862.
30. Zhou GM, Zhong ZS, Zhang LQ, et al. Experimental investigation on mechanical properties of hollow integrated sandwich composites. *J Nanjing Univ Aeronaut Astronaut* 2007; 39: 11–15 [in Chinese].
31. Papa E, Corigliano A and Rizzi E. Mechanical behaviour of a syntactic foam/glass fiber composite sandwich: experimental results. *Struct Eng Mechanic* 2001; 12(2): 169–188.
32. Bardella L and Genna F. Elastic design of syntactic foamed sandwiches obtained by filling of three-dimensional sandwich-fabric panels. *Int J Solid Struct* 2001; 38(2): 307–333.
33. Karahan M, Lomov S, Bogdanovich V, et al. Internal geometry evaluation of non-crimp 3D orthogonal woven carbon fabric composite. *Compos Part A* 2010; 41: 1301–1311.
34. Throne JL, Progelhof RC. Impact stress-strain behaviour of low density closed-cell foam. In: *Antec 85, Conference Proceedings for the Society of Plastics Engineers, Inc. 43rd Annual Technical Conference*. Washington D.C., USA, April 29–May 2, 1985, pp.442–446.
35. Rothschild Y, Echtemeyer AT and Arnesen A. Modelling of the non-linear material behaviour of cellular sandwich foam core. *Composites* 1994; 25(2): 111–117.
36. Grenestedt GL. Effective elastic behavior of some models for perfect cellular solids. *Int J Solid Struct* 1999; 36: 1471–1501.
37. Li QM, Mines RAW and Birch RS. The crush behavior of Rohacell-51 WF structural foam. *Int J Solid Struct* 2000; 37: 6321–6341.
38. Koissin V and Shipsa A. Mechanical properties of precompressed and undamaged Divinycell H-grade foam core. Report C2001-5, Department of Aeronautics, Royal Institute of Technology, Stockholm, 2001.
39. Gibson LJ and Ashby MF. *Ce1lular so1ids-structure and properties*. Oxford: Pergamon Press, 1988.
40. Zhang J and Ashby MF. Out-of-plane properties of honeycombs. *Int J Mech Sci* 1992; 34(6): 475–489.
41. Koissin V and Shipsha A. Deformation of foam cores uniaxial compression-tension cycle. In: *Proceedings of the 7th International Conference Sandwich Structures*, Aalborg University, Aalborg, Denmark, 29–31 August 2005.
42. Zhou GM, Zhong ZS, Zhang LQ, et al. Experimental investigation on mechanical properties of hollow integrated sandwich composites. *J Nanjing Univ Dept Aeronaut Astronaut* 2007; 39: 11–15.
43. Fan HL, Meng FH and Yang W. Mechanical behaviors and bending effects of carbon fiber reinforced lattice materials. *Arch Appl Mech* 2006; 75: 635–647.